Journal of Computational and Applied Research in Mechanical Engineering
jcarme.sru.ac.ir
SRTTU
JCARME
ISSN: 2228-7922

Research Paper

Study of the effect of the boundary layer excitation in the nanofluids flow inside the tube on increasing the heat transfer coefficient

J. Zareei[a,*], S. H. Hosseini[b] and M. Elveny [c]

[a]*Department of Biosystem Engineering, Ferdowsi University of Mashhad, Mashad, Iran*
[b]*Department of Mechanical Engineering, Islamic Azad University, Kashmar branch, Kashmar, Iran*
[c]*DS & CI Research group, Universitas Sumatera Utara, Medan, Indonesia*

Article info:

Article history:

Received: 29/11/2019
Accepted: 20/09/2021
Revised: 22/09/2021
Online: 25/09/2021

Keywords:
Nanofluid,
Nanoparticles,
Carbon nanotube,
Aluminumoxide nanoparticles,
Heat transfer coefficient.

[*]Corresponding author:
javadzareei@um.ac.ir

Abstract

In this paper, the effect of boundary layer excitation on increasing the heat transfer coefficient of water/carbon nanotube (CNT) nanofluid and water/aluminum oxide (Al_2O_3) nanoparticles has been investigated. The turbulent flow equations inside the pipe with RNG K-ε turbulence model are solved employing fluent software. The results show that the use of water/CNT nanofluid significantly increases the heat transfer coefficient of the convection. There is no such increase for water-aluminum oxide nanoparticles. If the volumetric percentage of the carbon nanotube increases, the rate of increase in the heat transfer coefficient and the flow pressure drop will increase. Therefore, the use of water/CNT nanofluid with lower volumetric percentages is better for improving the convective heat transfer. Also, by placing the barrier on the inner wall of the tube and stimulating the boundary layer, the heat transfer coefficient thereafter increases in the excitement area. In the present study, the use of three obstacles behind each other has increased the average heat transfer coefficient by 16.7%.

1. Introduction

To economically save and optimize systems used in industries such as electronic and space industries, it is necessary to design and produce small dimensional heat exchangers which are lightweight and have high efficiency. There are several ways to increase the heat transfer in this kind of equipment. The use of nanofluids, which is a mixture of solid particles with nano dimensions in the operating fluid, is considered as one of the newest and advanced methods for increasing the thermal conductivity of conventional fluids.

Another method is to put an obstacle in the flow path, which reduces the heat transfer rate by reducing the thickness of the heat boundary layer, to mix the flow and increase the heat transfer rate.

Laboratory studies have shown that nanofluids not only increase the thermal conductivity but also increase the convection heat transfer coefficient compared to the base fluid [1-2]. In addition to the laminar flow [3-5] laboratory review, some researchers have investigated the laboratory turbulent flows of nanofluids [6-9].

In addition to laboratory studies, some have studied the theory and numerical simulation of the flow and heat transfer of nanofluids in a laminar flow [10] and a turbulent flow [11]. Few studies have been carried out on the simulation of the turbulent flow of nanofluids. Namburu et al. [12] simulated a turbulent convection for three different nanofluids of CuO, Al_2O_3 and SiO_2 nanoparticles in a mixture of water and ethylene glycol. In this simulation, the turbulence model of RNG K-ε has been used for a turbulent flow inside a fixed heat flux pipe. The results showed that nanofluids containing CuO nanoparticles increased the heat transfer. Lotfi et al. [13-15] used the k-ε model to simulate the shifting of the water/Al_2O_3 nanofluid, inside a pipe, with static thermal flux conditions. They showed that nanofluid increases the Nusselt number and decreases the wall temperature. Some researchers have examined the effects of radiation on the heat transfer of nanofluids [16-18].

In numerical simulations of nanofluids, there are two methods to model the governing equations. In some references, the nanofluid is a logical fluid. In this case, the nanofluid is considered as a two-phase mixture, and two solid and liquid phases are analyzed individually. Most researchers, however, assume that the solid and base fluid nanoparticles are in equilibrium with heat and speed, considering the nanofluid as a single-phase environment. The assumption of a single-phase environment depends on the very small size of the nanoparticles and their very low volume fraction in the normal nanofluid; and all the equations governing the ordinary fluid for the nanofluid are also present. In this case, the effect of the nanoparticles in the fluid is chosen by selecting the proper effective properties for the nanofluid in the governing equations. This single-phase modeling is simpler than the two phases and is faster in terms of computing time.

Heat transfer improves when the hybrid-nanofluid rather than an ordinary nanofluid is employed [19, 20]. The working nanofluid was Al_2O_3-water whose characteristics have been obtaind by khanafer and Vafaei's model [21] which is a variable properties model.

Heat transfer characteristics of copper nanofluids with and without acoustic cavitation were studied experimentally. The results showed that the copper nanoparticles and acoustic cavitation had profound and significant influence on heat transport in the fluid [22, 23].

Also an investigation on convective heat transfer in elliptical pipes showed that 95% of the increase in the Nusselt number to the circular cylinder is related to an aspect ratio equal to 18.36; and carbon nanotubes reduce the damaged area. Skin friction coefficient and local Nusselt number can be reduced by magnetic field parameter and they can be enhanced by increasing the aligned angle [24-26].

The heat transfer phenomenon is very important in heat exchangers and in most heat exchangers it is used from the pipe. Therefore, the geometry of the studied tube is chosen in this study.

In the present study, the heat transfer of the convection in a turbulent flow of nanofluids passing through a tube without excitation of the boundary layer and along with the excitation of the boundary layer has been studied. Nanofluids used include cylindrical nanoparticles of carbon called carbon nanotubes (CNT), as well as aluminum oxide nanoparticles (Al_2O_3) in water base fluid. The turbulent flow equations with RNG K-ε turbulence model are solved employing fluent software. Also, this study shows that to reduce the heat transfer surface and reduce the dimensions of heat exchangers or to build a small heat exchanger with high heat efficiency, it is necessary to increase the transfer heat transfer coefficient. Stimulation of the boundary layer and the use of appropriate nanofluids can be used as an effective method to increase the thermal efficiency in such cases.

2. Flow modeling and heat transfer of nanofluids

In this research, the turbulent flow of water/CNT nanofluid and water/Al_2O_3 nanofluid with different percentages of nanoparticles passing through a tube has been investigated. The effect of nanoparticles has been entered by correction

of effective properties into the equations. These characteristics are: density, thermal capacity, dynamic viscosity, and thermal conductivity coefficient as determined below.

2.1. Density

According to the review of the existing reports, the density of nanofluids is calculated with the help of a classic model of mixture of two liquid-solid phases.

$$\rho_e = (1-\phi)\rho_f + \phi\rho_p \quad (1)$$

In this equation, ρ and ϕ represent the density and volumetric fraction of nanoparticles, respectively; and the subscripts f, p, and e indicate the properties of base fluid, nanoparticle, and nanofluid.

2.2. Heat capacity

Most researchers apply the following equation to the heat capacity of nanofluids.

$$C_{pe}(\emptyset\ T) = \frac{(1-\emptyset)\left(\rho(T)C_p(T)\right)_f + \emptyset(\rho C_p)_\rho}{(1-\emptyset)\rho_f(T) + \emptyset\rho_p} \quad (2)$$

2.3. Dynamic viscosity

The existing classical models are not capable of predicting the dynamic viscosity of nanofluids. For this reason, the dynamic viscosity of nanofluids used in this study has been obtained by fitting the bend on the available experimental results. With the fitting of the bend on the data, the following equation is obtained for the dynamic viscosity of the water/Al_2O_3 nanofluid.

$$\frac{\mu_e}{\mu_f} = (1+12.084\,\phi - 641.25\phi^2 + 22811\phi^3) \quad (3)$$

The fitting of the bend on the data [27] suggests the following equation for the dynamic viscosity of water/CNT nanofluid.

$$\frac{\mu_e}{\mu_f} = (1+12.084\,\phi - 641.25\phi^2 + 22811\phi^3) \quad (4)$$

2.4. Thermal conductivity coefficient

The thermal conductivity coefficient used in this study, presented in [27], is based on the nanolayer model around the nanoparticles. In the above reference, different models for spherical and cylindrical nanoparticles are presented. According to these models, the thermal conductivity coefficient for nanoparticles containing spherical nanoparticles, such as Al_2O_3, is:

$$k_e = [(k_p - k_l)\emptyset k_l(2\gamma_1^3 - \gamma^3 + 1)(k_p + 2k_l)\gamma_1^3(\emptyset\gamma^3 k_l - k_f) + k_f)] \times [\gamma_1^3(k_p + 2k_l) - (k_p - k_i)\emptyset(\gamma_1^3 + \gamma^3 - 1]^{-1} \quad (5)$$

For thermal conductivity, nanofluids containing cylindrical nanoparticles such as CNT are:

$$= [(k_p - k_l)\emptyset k_l(2\gamma_1^2 - \gamma^2 + 1)(k_p + k_l)\gamma_1^2(\emptyset\gamma^2(k_l - k_f) + k_f)] \times [\gamma_1^2(k_p + k_l) - (k_p - k_l)\emptyset(\gamma_1^2 + \gamma^2 - 1]^{-1} \quad (6)$$

In these equations, K_p, K_f, and K_l are the thermal conductivity of the nanoparticle, the base fluid and the nanolayer, respectively. The parameters γ_1 and γ are defined as follows

$$\gamma_1 = 1 + \frac{h}{2a} \quad (7a)$$

$$\gamma = 1 + \frac{h}{a} \quad (7b)$$

where "a" is the radius of the sphere or cylinder and "h" is the thickness of the nanolayer.
In the above equations, the properties of base fluid and nanoparticles are known. The only unknown factor is the thermal conductivity of the nanolayer (k_1) and the thickness of the nanolayer (h). According to [28], the value of nanolayer thickness for spherical Al_2O_3 particles is 1nm and for CNT cylindrical particles is 2nm. The thermal conductivity of the nanolayer is obtained from its compliance with laboratory results. Thus, the nanotube thermal conductivity coefficient for spherical Al_2O_3 particles with a diameter of 30 nm is obtained according to reference laboratory data [29-31] equal to K_1 =

1.5K_f . Similarly, for CNT cylindrical particles with a diameter of 15nm and a length of 30μm, the thermal conductivity of the nanolayer is equal to $K_1 = 555K_f$.

3. Numerical solution of flow equations

In this paper, incompressible turbulent flow equations inside a pipe are solved by using the k-ε two-state turbulence model by means of the fluent software. To reduce the computational volume and use a smaller number of computational cells, a quarter of the tube is modeled. For this purpose, according to Fig.1(a) and Fig.1(b), a highly regulated network is created using four-sided cells.

In order to stimulate the boundary layer and create turbulence in the flow of fluid, various barriers are installed inside the pipe. Barriers are at a distance of 40 cm from the entrance to the pipe. The barriers are used in the form of donuts with circle and triangle sections.

In Fig. 2, the two barriers used are shown. In this figure, a distance of 7 cm from the tube where barriers are located is shown. First, the initial part of the tube, which has no barrier, is solved separately and its results are solved using the profiles of the velocity, temperature, and turbulence intensity to the input of this part of the pipe which has a barrier. This technique has been used to reduce the solving time. Also, using this technique can consider more obstacles with less computational cost.

Due to the huge importance of calculating gradients near the pipe wall, networking is in the vicinity of the pipe wall. In order to validate the numerical solution and investigate the effect of the computational network on the solution results, the Nusselt number is used. The Nusselt number is obtained from the Dittus-Boelter equation in a completely developed flow within the pipe:

$$N_{uD} = 0.023 Re_D^{4/5} Pr^{0.3} \quad (8)$$

where Re_D is the Reynolds number and Pr is Prandtl number. In order to compare the simulation results with the Nusselt number obtained from the above equation, the pipe length should be considered sufficiently long.

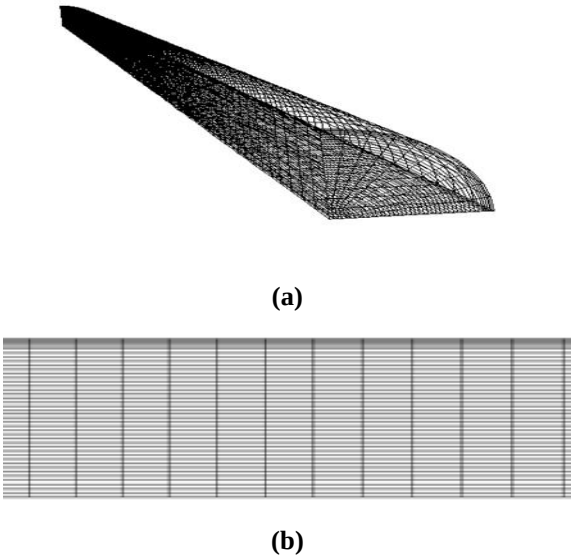

(a)

(b)

Fig. 1. (a) Tube geometry and networking solution environment, and (b) Computational grid(10000 Cell mesh) on symmetry plane (The network adjacent to the wall).

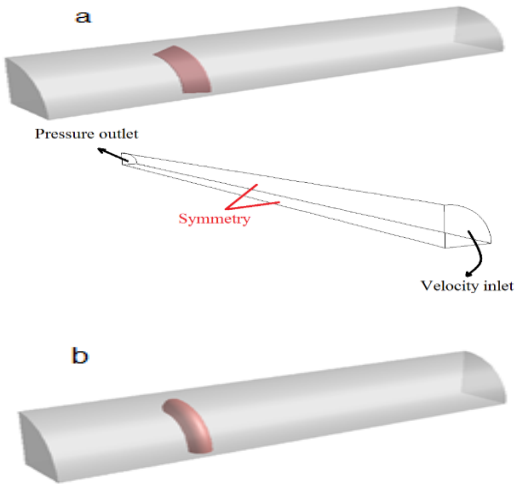

Fig. 2. Barriers used to stimulate flow in the pipe, (a) a barrier with a triangular cross section and (b) a barrier with a circular cross section.(D=19mm, L= 39 cm)

The developmental length in the turbulent flow inside the tube (L) is obtained from the following equation.

$$\frac{L}{D} = 4{,}4 Re_D^{1/6} \quad (9)$$

In order to validate the numerical solution and to check the independence of the results from the computational network, a flow of air at a speed

of 8 m/s and a temperature of 350 k inside the pipe with diameter of 19 mm (3/4 inches) is considered (the tube wall temperature is considered to be 273k); some characteristics are mentioned in Table 1. By calculating the Reynolds and Pranlet number for air flow and using Eqs. (8 and 9), the Nusselt number and the developmental length of the flow are 34.4 and 0.39 m, respectively. Therefore, in the numerical solution, the length of the pipe is 39 cm. In Fig. 3, the distribution of Nusselt number is presented in terms of pipe length for a network of different sizes. The height of the first computational cell adjacent to the pipe wall for each computational network is specified in this figure. In addition, the value of the Nusselt number in the fully developed state is specified.

As can be seen, by shrinking the first computational cell adjacent to the tube wall, the Nusselt number gets nearer and closer to the Nusselt number at the end of the pipe, as far as 0.1 mm in size, with an error less than 3% overlap. In this case, the error rate of the Nusselt number compared to the value obtained from the Dittus-Boetler equation is less than 2.2%. Therefore, the size of the cells in the computing network is 0.1 millimeters to continue the work. Therefore, the results of Nusselt number with scales of 0.1 and 0.2 show that there is a small computational error so that in this case the calculations of Nusselt number can be considered independent of the mesh.

Fig. 3 is used to select the appropriate mesh network size. For this purpose, the NuD number in the fully developed flow of the tube is calculated in the developmental length (L) and its values are 34.4 and 39 cm, respectively. Then for a pipe with length 39 cm in numerical method and for a grid of different sizes, the Nusselt number of the pipe is calculated from the beginning of the tube to the end in different lengths. Finally, the value obtained at the end of the pipe (39 cm long, Fully Developed Flow) is compared in two ways, as described in Table 2. Accordingly, the size of the network is 0.1 mm, and the rest of the calculations are done with this size.

3.1. Validation model

To predict the increase in surface heat transfer during the use of nanofluids, both numerical and experimental methods have been used. As shown in Fig. 4, in both methods, with the increase in the percentage of carbon nanotubes in water, the ratio of the surface heat transfer coefficient of nanofluid (SHTC) to the surface heat transfer coefficient of pure water (SHTCp) increases.

Table 1. Geometric characteristics and boundary conditions

Quantity	Value
Pipe diameter	19 mm
length of the pipe	39 cm
Intake air velocity	8 m/s
Inlet air temperature	350 K
Tube wall temperature	273 K

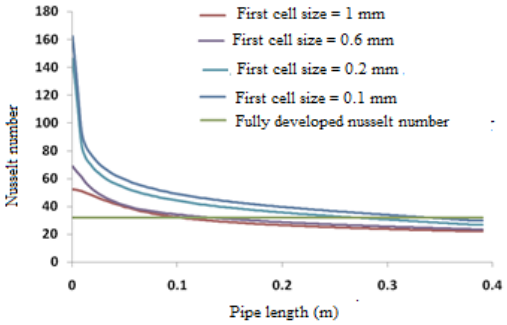

Fig. 3. Distribution of Nusselt number of the tube wall according to pipe length in different networks.

Table 2. The error value of the Nusselt number compared to the value obtained from the dittus-boetler relationship.

The size of the first cell adjacent to the tube wall	Percentage error
1 mm	16.5
0.5 mm	11.1
0.2 mm	4.1
0.1 mm	2.2

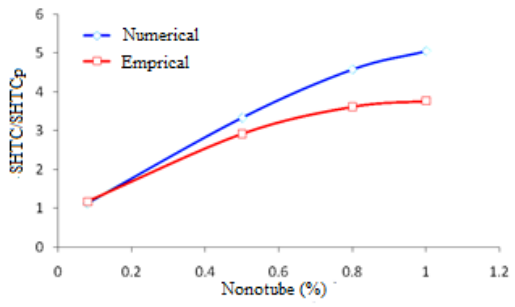

Fig. 4. Changes in the ratio of the surface heat transfer coefficient of nanofluid (SHTC) to surface heat transfer coefficient of pure water (SHTCp) for different CNTs concentrations by numerical and experimental models.

This increase rate is reduced by increasing the percentage of nanoparticles as with increasing nanotube percentage from 0.8 to 1%, the increase in heat transfer coefficient does not change considerably. On the other hand, by increasing the CNT concentration, the difference between numerical and experimental results increases. This can be related to the type of simulation and the use of a single-phase environment for a nanofluid and the assumption of thermal and velocity equilibrium between solid and base fluid nanoparticles. In fact, single phase modeling simplifies the computation rather than two phases and accelerates the calculation time, but causes a slight difference between numerical and experimental results, especially in high concentration of the nanoparticles (Fig. 4).

4. Results and discussion

4.1. The effect of the boundary layer excitation on fluid dynamics and heat transfer coefficient

After ensuring the correctness of the numerical solution and choosing the appropriate network size, the turbulent flow equations in the pipe are solved for pure water at an input speed of 2 m / s and a temperature of 350 k. The tube wall temperature is considered to be 273 Kelvin. To stimulate the boundary layer and create turbulence in the flow of fluid, two different barriers are used, one with a circle cross section, and the other a triangle that is used in the form of donuts inside the pipe. First, the equations in the elementary part of the tube without an obstacle are solved separately, and the results are presented for the speed, temperature, and turbulence profiles of the pipe entrance which has an obstacle. This technique has been used to reduce the solving time. Also, using this technique, one can consider more obstacles with less computational cost. In Figs. 5 and 6, the distribution of the velocity around the barrier with a circular and triangular cross section is shown. The flow direction is from the right to the left. As can be seen, a jet has been created from the fluid in the vicinity of the barrier and a long vortex in the back of the barrier. The maximum speed has reached more than four meters per second. The triangular barrier, in comparison to the circular barrier, guides the flow better to the wall of the pipe, and the length of the fluid jet created is louder, but the maximum velocity is less than the circular barrier. Increasing the velocity of the fluid in the vicinity of the wall reduces the thickness of the boundary layer and increases the gradient and increases the shear stress of the wall and the pressure drop. In Fig. 7, the distribution of the heat transfer coefficient of convection of the tube wall is shown in two states of circular barrier and triangular barrier.

In both barriers, the heat transfer coefficient increases significantly with the arrival of the fluid. By passing the fluid through the barrier, the heat transfer coefficient gradually decreases[32, 33]. As can be seen, an increase in the heat transfer coefficient of the tube wall in the area around the barrier (excitation zone) in the case of a barrier with a triangular cross section is more than the circular barrier.

When facing, the flow is created through barriers of a jet in the vicinity of the pipe wall and a vortex on the back of the barrier. Increasing fluid velocity in the vicinity of the wall reduces the thickness of the boundary layer and increases the shear stress of the wall. For this reason, the use of the barrier while increasing the heat transfer coefficient also increases the pressure drop.

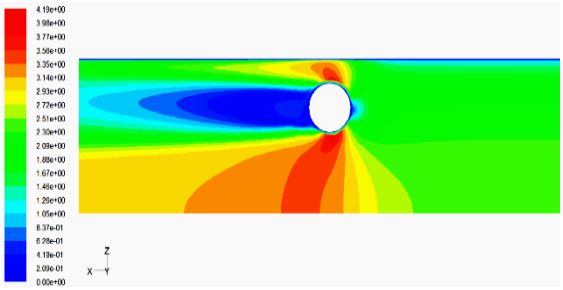

Fig. 5. Distribution of the velocity around the obstacle with a circular cross section on the symmetry plate.

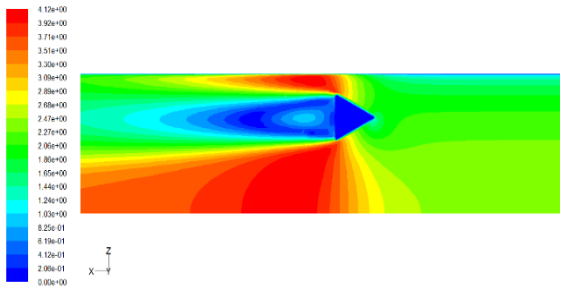

Fig. 6. Distribution of the velocity around the obstacle with a triangular cross section on the symmetry plate.

For a slightly better comparison, in Table 3, the average value of the heat transfer coefficient of the tube wall and the flow pressure drop in unobstructed state with two barriers are compared. The comparison of the numbers in Table 3 shows that the triangular barrier increases the heat transfer coefficient more than the other two, but instead, a higher pressure drop will flow.

In Fig. 8, the thermal transfer coefficient of the tube wall is shown in terms of length for pure water and water/CNT nanofluids with different percentages. As expected, increasing the percentage of carbon nanotubes in the water increases the convection heat transfer coefficient.

Due to the formation of a vortex in the back of the barrier, a second partial maximum point is generated in the heat transfer coefficient graph, which increases its rate by increasing the percentage of carbon nanotubes.

In Fig. 9, the distribution of the convection heat transfer coefficient of the tube wall is compared to the pure water for water/AL_2O_3 nanofluid. As can be seen, the heat transfer coefficient of the wall slightly increases compared to water, but this increase is negligible compared to water/CNT nanofluid. Therefore, the use of this nanofluid does not significantly change the heat transfer coefficient of the tube wall. The main reason for this subject can be related to the coefficient of the low thermal conductivity of aluminum oxide nanoparticles compared to carbon nanotubes. In Table 4, can see the Properties of nanoparticles and different nanofluids.

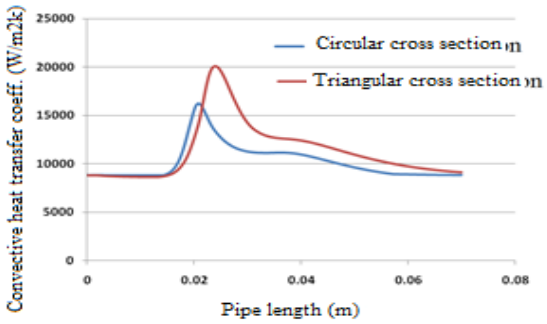

Fig. 7. Comparison of the distribution of the convection heat transfer coefficient in terms of pipe length of the circular and triangular barrier.

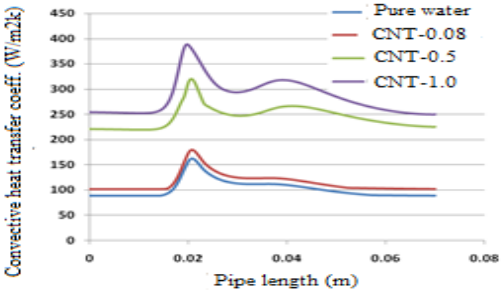

Fig. 8. Distribution of the heat transfer coefficient of tube wall for water/CNT nanofluids with different percentages.

Table 3. Pressure drop and heat transfer coefficient in three different conditions.

Type of tube	Average heat transfer coefficient (W/m2K)	Pressure drop(Pa)
Unobstructed tube	8851	203
Barrier with circular cross section	10150	1782
Barrier with triangular cross section	11462	3424

Table 4. Properties of nanoparticles and different nanofluids used.

Material		ρ Kg/m^3	C_p J/(kg.k)	μ (pa.s)	K w/(m.k)	Pr
Al2O3		3970	765	-	36	-
CNT		2600	425	-	3000	-
Water		1000	4183	0.85×10-3	0.6	5.93
Water / Al2O3	1%	1029.7	4051	0.92×10-3	0.62	6.07
	4%	1119	3698	1.26×10-3	0.67	7
Water / CNT	0.08%	1001	4175	0.85×10-3	0.72	4.93
	0.5%	1008	4134	0.87×10-3	3.7	0.97
	1%	1016	4087	1.1×10-3	7.84	0.61

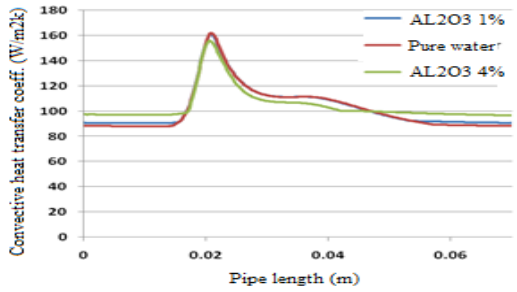

Fig. 9. Distribution of the heat transfer coefficient of the wall according to the pipe length for water/AL_2O_3 nanofluid.

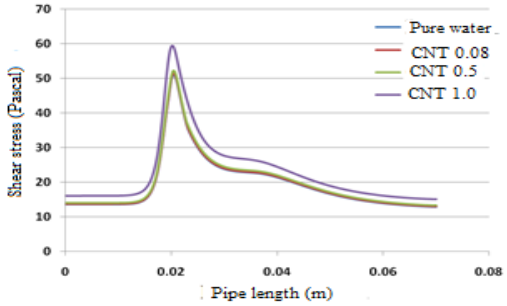

Fig. 10. Shear stress distribution of tube wall for pure water and water/CNT nanofluid with different percentages.

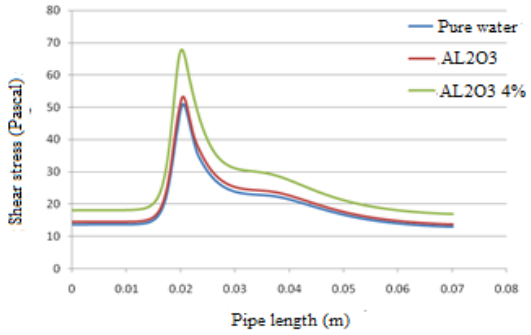

Fig. 11. Shear stress distribution of tube wall for pure water and water/AL_2O_3 nanofluid with different percentages.

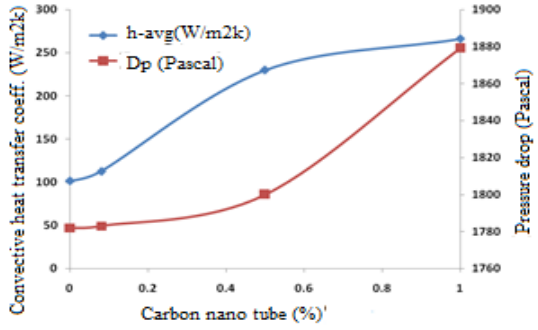

Fig. 12. The average heat transfer coefficient of the wall and the pressure drop in water/CNT nanofluid with different percentages.

In Fig. 10, the shear stress distribution of the pipe wall for pure water and water/CNT nanofluid with different percentages of nanotubes is shown; also in Fig. 11, the distribution of shear stresses for pure water and water/AL_2O_3 nanofluid is depicted. As can be seen, the shear stress of the tube wall for 4% water/AL_2O_3 nanofluid is maximum. Despite the fact that water/AL_2O_3 nanofluid do not increase the value of the heat transfer to the wall, it greatly increases the shear stress of the wall, resulting in lowering the pressure of the flow, and therefore its use does not seem appropriate.

In Fig. 12, the average heat transfer coefficient of the tube wall as well as the value of the pressure drop in water/CNT nanofluid is drawn as a percentage of carbon nano tube (CNT). As can be seen, both graphs have an ascending trend, but with increasing CNT percentages from 0.5% to 1%, the pressure drop has increased sharply while the heat transfer coefficient has not increased significantly. Therefore, the use of this nanofluid with a low volumetric CNT content is more suitable for better heat transfer.

In Figs. 13 and 14, the distribution of the velocity of the fluid in the two-plate symmetry and the distribution of the heat transfer coefficient of the wall are shown in terms of the length of the pipe in the presence of three barriers of the shape of the donut with a circular cross section. As can be seen, the velocity of the fluid increases through each barrier and then decreases again. Increasing the flow velocity at the distance between the barrier and the tube wall and causing the jet to form a fluid in that area greatly increases the heat transfer coefficient of the pipe wall, so that the heat transfer coefficient in the vicinity of all three obstacles has increased sharply.

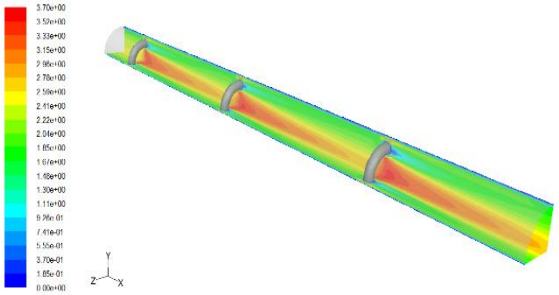

Fig. 13. Distribution of velocity in symmetry plates.

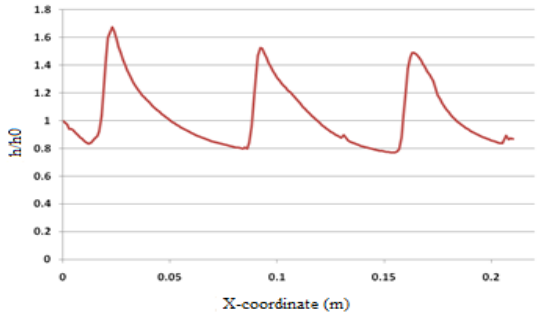

Fig. 14. Distribution of the convection heat transfer coefficient in terms of the length of the pipe in the presence of three barrel shapes of the donut with a circular cross section.

The intensity of excitement decreases in the first and further obstacles, and with the progression along the tube, the intensity of excitation is reduced by obstacles. Before each obstacle due to the stagnation point created on the barrier, the fluid velocity is slightly reduced, resulting in a slight reduction in the heat transfer coefficient. In sum, the use of three continuous barriers in the flow direction the average heat transfer coefficient increased by 16.7%.

5. Conclusions

In this study, nanofluids containing the mixture of carbon nanotube (CNT) in cylindrical particles and aluminum oxide nanoparticles (Al_2O_3) in base fluid (water) in turbulent flow of the tube in two conditions of existence and no barrier have been studied. Turbulent flow equations with RNG K-ε turbulence model are solved employing fluent software.

- The results show that the use of nanofluid containing carbon nanotubes and water alone would significantly increase the heat transfer coefficient of the tube wall , where there was no such increase for aluminum oxide nanoparticles and water.
- with the increase in the percentage of carbon nanotubes in water, the ratio of the surface heat transfer coefficient of the nanofluid surface (SHTC) to the pure water surface heat transfer coefficient of pure water (SHTCp) increases. This increase rate is reduced by increasing the percentage of nanoparticles as with increasing nanotube percentage from 0.8 to 1%, the increase in heat transfer coefficient does not change considerably .
- The shape of the barrier has a significant effect on the degree of excitation of the boundary layer and the formation of turbulence. A comparison of the use of triangular and circular barriers shows that the increase in the heat transfer coefficient of the tube wall in the area around the barrier (excitation zone) in the case of a barrier with a triangular cross section is more than the circular barrier.
- Increasing fluid velocity in the vicinity of the wall reduces the thickness of the boundary layer and increases the shear stress of the wall. For this reason, the use of the barrier while increasing the heat transfer
  coefficient also increases the pressure drop. As the velocity of the fluid increases near the wall, both the pressure drop and the heat transfer coefficient increase.
- The increase in the first barrier has been high and gradually decreases in the next barriers. In the present study, the use of three barrier obstacles increased the average convection heat transfer coefficient of 16.7%. Also, the heat transfer coefficient increases slightly and the pressure drop is significant, when water/Al2O3 nanofluid is on the contrary.
- An increase in the volumetric CNT content in water for low percentages causes a rapid increase in the heat transfer coefficient and partial pressure drop in the flow. However, for high percentages, an increase in the CNT percentage causes a slight increase in the heat transfer coefficient and a rapid increase in the pressure drop in the flow. Therefore, the use of nanofluid with a low volumetric CNT content is more suitable for improving the heat transfer.

References

[1] K. Nishant and S. S. Sonawans, "Experimental study of thermal conductivity and convective heat transfer enhancement using CuO and TiO_2 nanoparticles", *Int. J. Heat. Mass. Transf*, Vol. 76, No. 1, pp. 98-107, (2016).

[2] M. Khoshvaght-Aliabadi, S. M. Hassani and S. H. Mazloumi, "Comparison of hydrothermal performance between plate fins and plate-pin fins subject to nanofluid-cooled corrugated miniature heat sinks", *Mic. Reli*, Vol. 70, No. 1, pp. 84-96, (2017).

[3] H. Chen, W. Yang, Y. He, Y. Ding, L. Zhang, Ch. Tan, A.A. Lapkin and D.V. Bavykin, "Heat transfer and flow behaviour of aqueous suspensions of titanate nanotubes (nanofluids)", *Pow. Tech*, Vol. 183, No. 1, pp. 63–72, (2008).

[4] K. B. Anoop, T. Sundararajan and S. K. Das, "Effect of particle size on the convective heat transfer in nanofluid in the developing region", *Int. J. Heat. Mass. Trans*, Vol. 52, No. 9-10, pp. 2189–2195, (2009).

[5] K. S. Hwang, S. P. Jang and S. Choi, "Flow and convective heat transfer characteristics of water-based Al2O3 nanofluids in fully developed laminar flow regime", *Int. J. Heat. Mass. Trans*, Vol. 52, No. 1-2, pp. 193–199, (2009).

[6] W. C. Williams, J. Buongiorno and L. W. Hu, "Experimental investigation of turbulent convective heat transfer and pressure loss of alumina/water and zirconia/water nanoparticle colloids (nanofluids) in horizontal tubes", *ASME J. Heat. Trans*, Vol. 130, No. 4, pp. 1-6, (2008).

[7] B. Farajollahi, S. Gh. Etemad and M. Hojjat, "Heat transfer of nanofluids in a shell and tube heat exchanger", *Int. J. Heat. Mass Trans*, Vol. 53, No. 1-3, pp. 12–17, (2010).

[8] S. M. Fotukian and M. Nasr Esfahany, "Experimental investigation of turbulent convective heat transfer of dilute c-Al2O3/water nanofluid inside a circular tube", *Int. J. Heat. Fluid. Flow*, In Press, Vol. 31, No. 4, pp. 606-612 (2010).

[9] W. Duangthongsuk and S.Wongwises, "Comparison of the effects of measured and computed thermophysical properties of nanofluids on heat transfer performance", *Ex. Ther. Flui. Sci*, Vol. 34, No. 5, pp. 616–624, (2010).

[10] A. Akbarinia and A. Behzadmehr, "Numerical study of laminar mixed convection of a nanofluid in horizontal curved tubes", *Appl. Therm. Eng*, Vol. 27, No. 8-9, pp. 1327–1337, (2007).

[11] M. Khoshvaght-Aliabadi, S. M. Hassani and S. H Mazloumi. "Comparison of hydrothermal performance between plate fins and plate-pin fins subject to nanofluid-cooled corrugated miniature heat sinks", *Mic. Reli*, Vol. 70, No. 1, pp.84-96, (2017).

[12] P.K. Namburu, D. K. Das, K.M.Tanguturi and S. Vajjha, "Numerical study of turbulent flow and heat transfer characteristics of nanofluids considering variable properties", *Int. J. Ther. Sci*, Vol. 48, No. 2, pp. 290–302, (2009).

[13] R. Lotfi, Y. Saboohi and A. M. Rashidi, "Numerical study of forced convective heat transfer of Nanofluids: Comparison of different approaches", *Int. Co. Heat. Mass Trans*, Vol. 37, No. 1, pp. 74–78, (2010)

[14] P. Valipour, R. Moradi and F. Shaker Aski, "CNT-water nanofluid thermal radiation heat transfer over a stretching sheet considering heat generation", *J. Mol. li*, Vol. 237, No. 1, pp. 242-246, (2017).

[15] A. S. Dogonchi and D. D. Ganji, "Impact of Cattaneo-Christov heat flux on MHD nanofluid flow and heat transfer between paraller plates considering thermal radiation effect", *J. Tai. Ins. Che. Eng*, Vol. 80, No. 1, pp.52-63 (2017).

[16] D. Zhou, "Heat transfer enhancement of copper nanofluid with acoustic cavitation", *Int. J. Heat. Mass. Trans*, Vol. 47, No. 14-16, pp.3109-3117,(2004).

[17] R. Saidur, K. Y. Leong and Ha Mohammad, "A review on applications and challenges of nanofluids",Renew. *Sus. Ener. reviews*, Vol. 15, No. 3, pp. 1646-1668, (2011).

[18] K. Khanafer and K. Vafai, "A critical synthesis of thermophysical characteristics of nanofluids", *Int. J. Heat. Mass. Trans*, Vol. 54, No. 19-20, pp. 4410-4428, (2011).

[19] A. Akbar Rashidi and E. Kianpour, "Investigation of natural convection heat transfer of MHD hybrid nanofluid in a triangular enclosure," *J. Comput. Appl. Res. Mech. Eng* (JCARME), Vol. 10, No. 2 pp. 539-549. (2018).

[20] E. M. Hemmat, M. Akbari A. Karimipour, M. Afrand, Omid Mahian and Somchai Wongwises, "Mixed-convection flow and heat transfer in an inclined cavity equipped to a hot obstacle using nanofluids considering temperature-dependent properties", *Int. J. Heat. Mass Trans*, Vol. 85, No. 1, pp. 656-666 (2015).

[21] A. Chamkha and E. Abu-Nada, "Mixed convection flow in single-and double-lid driven square cavities filled with water–Al2O3 nanofluid: Effect of viscosity models", *European J. Mech. B/Flui*, Vol. 36, No. 1, pp. 82-96, (2012).

[22] T. Adibi, "Three-dimensional characteristic approach for incompressible thermo-flows and influence of artificial compressibility parameter", *J. Comp. Appl. Re. Mech. Eng, (JCARME)* Vol. 8, No. 2, pp. 223-234, (2019).

[23] S. Ahmadipour, M. H. Aghkhani and J. Zareei, "Investigation of injection timing and different fuels on the diesel engine performance and

emissions", *J. Comput. Appl. Res. Mech Eng (JCARME*), Vol. 9, No. 2, pp.385-396 (2019).
[24] M. M. Shahmardan, M. Norouzi and M. H. Sedaghat, "An Exact Analytical Solution for Convective Heat Transfer in Elliptical Pipes", *AUT J. mech. eng*, Vol. 1, No. 2, pp. 131-138 (2017).
[25] L. Chen, H. Xie, Y. Li And W. Yu, "Nanofluids containing carbon nanotubes treated by mechanochemical reaction", *Therm. Acta*, Vol. 477, No 1-2, pp. 21–24, (2008).
[26] S. Murshed, K. Leong and C. Yang, "Investigations of thermal conductivity and viscosity of nanofluids", *Int. J. Therm. Sci*, Vol. 47, No. 5, pp. 560–568, (2008).
[27] H. S. Xue, J. R. Fan, R. H. Hong and Y. C. Hu, "Characteristic boiling curve of carbon nanotube nanofluid as determined by the transient calorimeter technique", *Appl. Phy.Let*, Vol. 90, No. 18, pp. 184107, (2007).
[28] J. Zareei, A. Rohani and W. Mohd, "effect of ignition an injection timing along with hydrogen enrichment to natural gas in a direct injection engine on performance and exhaust emission", *Int. J. Auto. Eng*, Vol. 8, No. 1, pp. 2614-2632, (2018).
[29] A. Kakaee and J. Zareei, "Influence of varying timing angle on performance of an SI engine: An experimental and numerical study", *J. Comp. Appl. Res. Mech. Eng* (JCARME), Vol. 2, No. 2, pp. 33-43, (2013).
[30] S. Murshed, K. Leong and C. Yang, "Investigations of thermal conductivity and viscosity of nanofluids", *Int. J. Therm. Sci*, Vol. 47, No. 5, pp. 560–568, (2008).
[31] H. S. Xue, J. R. Fan, R. H. Hong and Y. C. Hu, "Characteristic boiling curve of carbon nanotube nanofluid as determined by the transient calorimeter technique", *Appl. Phy.Let*, Vol. 90, No. 18, pp. 184107, (2007).
[32] J. Zareei, A. Rohani and W. Mohd, "effect of ignition an injection timing along with hydrogen enrichment to natural gas in a direct injection engine on performance and exhaust emission", *Int. J. Auto. Eng*, Vol. 8, No. 1, pp. 2614-2632, (2018).
[33] A. Kakaee and J. Zareei, "Influence of varying timing angle on performance of an SI engine: An experimental and numerical study", *J. Comp. Appl. Res. Mech. Eng* (JCARME), Vol. 2, No. 2, pp. 33-43, (2013).

How to cite this paper:

J. Zareei, S. H. Hosseini and M. Elveny, " Study of the effect of the boundary layer excitation in the nanofluids flow inside the tube on increasing the heat transfer coefficient", *J. Comput. Appl. Res. Mech. Eng.*, Vol. 12, No. 1, pp. 109-119, (2022).

DOI: 10.22061/JCARME.2021.6252.1795

URL: https://jcarme.sru.ac.ir/?_action=showPDF&article=1601